Check for updates

Time and Fourier domain jointly mode locked frequency comb swept fiber laser

MINGGUI WAN,[1,4] FENG LI,[2,3,4,5] XINHUAN FENG,[1,6] XUDONG WANG,[1] YUAN CAO,[1] BAI-OU GUAN,[1] DONGMEI HUANG,[2,3] JINHUI YUAN,[2,3] AND P. K. A. WAI[2,3]

[1]*Guangdong Provincial Key Laboratory of Optical Fiber Sensing and Communications, Institute of Photonics Technology, Jinan University, Guangzhou 510632, China*
[2]*The Hong Kong Polytechnic University Shenzhen Research Institute, Shenzhen 518057, China*
[3]*Photonics Research Centre, Department of Electronic and Information Engineering, The Hong Kong Polytechnic University, Hong Kong SAR, China*
[4]*These authors contributed equally*
[5]*enlf@polyu.edu.hk*
[6]*eexhfeng@gmail.com*

Abstract: Fourier domain mode locked (FDML) fiber lasers enable megahertz wavelength sweeping rate but suffer from the short coherent length. Discretization of the swept spectrum by a comb filter was demonstrated effective to enhance the coherent length. In this paper, we propose a novel discretization method of the FDML signal with an intracavity intensity modulator. We propose and successfully demonstrate a time and Fourier domain jointly mode locked fiber laser with a Fabry-Pérot comb filter and an intensity modulator in the cavity. A 50 GHz free spectral range comb filter in the Fourier domain mode locked fiber swept laser slices the spectrum into a series of comb lines and chops the swept signal into short pulses in time domain. The temporal signal is detected by a photodetector to generate a series of ultrashort pulses to drive the intensity modulator to further polish the intracavity pulses. We experimentally realized the proposed time and Fourier domain jointly mode locked fiber laser. Discrete wavelength swept laser output with a wavelength spacing of ~0.4 nm in a 41 nm sweeping range has been achieved.

© 2017 Optical Society of America under the terms of the OSA Open Access Publishing Agreement

OCIS codes: (140.3600) Lasers, tunable; (140.3510) Lasers, fiber; (140.4050) Mode-locked lasers.

References and links

1. K. Wijesundara, C. Zdanski, J. Kimbell, H. Price, N. Iftimia, and A. L. Oldenburg, "Quantitative upper airway endoscopy with swept-source anatomical optical coherence tomography," Biomed. Opt. Express **5**(3), 788–799 (2014).
2. T. Klein, W. Wieser, L. Reznicek, A. Neubauer, A. Kampik, and R. Huber, "Multi-MHz retinal OCT," Biomed. Opt. Express **4**(10), 1890–1908 (2013).
3. C. Ryu and C. Hong, "Development of fiber Bragg grating sensor system using wavelength-swept fiber laser," Smart Mater. Struct. **11**(1), 468–473 (2002).
4. D. P. Zhou, Z. Qin, W. Li, L. Chen, and X. Bao, "Distributed vibration sensing with time-resolved optical frequency-domain reflectometry," Opt. Express **20**(12), 13138–13145 (2012).
5. S. Jyu, S. Liu, W. Hsiang, and Y. Lai, "Fiber Dispersion Measurement With a Swept-Wavelength Pulse Light Source," IEEE Photonics Technol. Lett. **22**(9), 598–600 (2010).
6. M. Y. Jeon, N. Kim, S. P. Han, H. Ko, H. C. Ryu, D. S. Yee, and K. H. Park, "Rapidly frequency-swept optical beat source for continuous wave terahertz generation," Opt. Express **19**(19), 18364–18371 (2011).
7. S. H. Yun, C. Boudoux, G. J. Tearney, and B. E. Bouma, "High-speed wavelength-swept semiconductor laser with a polygon-scanner-based wavelength filter," Opt. Lett. **28**(20), 1981–1983 (2003).
8. R. Huber, M. Wojtkowski, K. Taira, J. Fujimoto, and K. Hsu, "Amplified, frequency swept lasers for frequency domain reflectometry and OCT imaging: design and scaling principles," Opt. Express **13**(9), 3513–3528 (2005).
9. B. Potsaid, B. Baumann, D. Huang, S. Barry, A. E. Cable, J. S. Schuman, J. S. Duker, and J. G. Fujimoto, "Ultrahigh speed 1050nm swept source/Fourier domain OCT retinal and anterior segment imaging at 100,000 to 400,000 axial scans per second," Opt. Express **18**(19), 20029–20048 (2010).
10. W. Wieser, B. R. Biedermann, T. Klein, C. M. Eigenwillig, and R. Huber, "Multi-Megahertz OCT: High quality 3D imaging at 20 million A-scans and 4.5 GVoxels per second," Opt. Express **18**(14), 14685–14704 (2010).

11. S. W. Lee, C. S. Kim, and B. M. Kim, "External Line-Cavity Wavelength-Swept Source at 850 nm for Optical Coherence Tomography," IEEE Photonics Technol. Lett. **19**(3), 176–178 (2007).
12. R. F. Stancu and A. G. Podoleanu, "Dual-mode-locking mechanism for an akinetic dispersive ring cavity swept source," Opt. Lett. **40**(7), 1322–1325 (2015).
13. H. D. Lee, Z. Chen, M. Y. Jeong, and C. S. Kim, "Simultaneous Dual-Band Wavelength-Swept Fiber Laser Based on Active Mode Locking," IEEE Photonics Technol. Lett. **26**(2), 190–193 (2014).
14. Y. Takubo and S. Yamashita, "High-speed dispersion-tuned wavelength-swept fiber laser using a reflective SOA and a chirped FBG," Opt. Express **21**(4), 5130–5139 (2013).
15. R. Huber, M. Wojtkowski, and J. G. Fujimoto, "Fourier domain mode locking (FDML): a new laser operating regime and applications for optical coherence tomography," Opt. Express **14**(8), 3225–3237 (2006).
16. R. Huber, D. C. Adler, and J. G. Fujimoto, "Buffered Fourier domain mode locking: Unidirectional swept laser sources for optical coherence tomography imaging at 370,000 lines/s," Opt. Lett. **31**(20), 2975–2977 (2006).
17. J. Zhang, J. Jing, P. Wang, and Z. Chen, "Polarization-maintaining buffered Fourier domain mode-locked swept source for optical coherence tomography," Opt. Lett. **36**(24), 4788–4790 (2011).
18. B. R. Biedermann, W. Wieser, C. M. Eigenwillig, T. Klein, and R. Huber, "Dispersion, coherence and noise of Fourier domain mode locked lasers," Opt. Express **17**(12), 9947–9961 (2009).
19. W. Wieser, T. Klein, D. C. Adler, F. Trépanier, C. M. Eigenwillig, S. Karpf, J. M. Schmitt, and R. Huber, "Extended coherence length megahertz FDML and its application for anterior segment imaging," Biomed. Opt. Express **3**(10), 2647–2657 (2012).
20. F. Li, K. Nakkeeran, J. N. Kutz, J. Yuan, Z. Kang, X. Zhang, and P. K. A. Wai, "Eckhaus Instability in the Fourier-Domain Mode Locked Fiber Laser Cavity", arXiv:1707.08304 [physics.optics], (2017).
21. T. H. Tsai, C. Zhou, D. C. Adler, and J. G. Fujimoto, "Frequency comb swept lasers," Opt. Express **17**(23), 21257–21270 (2009).
22. C. M. Eigenwillig, B. R. Biedermann, G. Palte, and R. Huber, "K-space linear Fourier domain mode locked laser and applications for optical coherence tomography," Opt. Express **16**(12), 8916–8937 (2008).

1. Introduction

Wavelength swept laser sources are enabling equipment in many applications such as spectroscopy, instrument test, optical fiber Bragg grating (FBG) sensing, optical frequency domain reflectometer (OFDR), and optical coherence tomography (OCT) [1–6]. OCT is currently a very important application of wavelength swept laser due to the continuously extending applications and the great potential market [7–10]. On the same time, OCT is also an application that has very strong requirement to the sweeping performance including sweep range, sweep rate, sweep linearity and coherence length. To enlarge the sweep range, semiconductor optical amplifiers (SOAs) with broad and flat gain profiles are normally used as the gain elements [11–14]. The sweep rate required by OCT is much higher than other applications. In an optical FBG sensing system, a sweep rate of several kHz or even sub-kHz is already enough for the interrogation [3, 4]. But such sweep rate is too low for swept source OCT, which needs a sweep rate at least larger than several tens of kHz for high speed imaging [1, 2]. The sweep rate of traditional short cavity swept laser is greatly limited by the laser build-up time in the new wavelength which normally needs kilo-roundtrips propagation in the cavity [7, 8]. Fourier domain mode locked (FDML) fiber laser provides a novel solution to avoid the rebuild of laser signal by inserting a long fiber to buffer the whole swept signal in the cavity with synchronization to the sweep rate of the filter [15]. With pulse stacking to boost the sweep rate, the effective sweep rate of FDML fiber laser has been improved to several MHz, which is much higher than other swept sources [16, 17]. The major problem or drawback that currently limits the performance of FDML fiber laser is the large instantaneous linewidth, or correspondingly a short coherent length [18, 19].

It is known that the dispersion of the long fiber in the FDML fiber laser cavity will lead to frequency offset between the signal and the swept filter. Recently we find that the Eckhaus instability caused by the interaction of the consecutive frequency shift and the confinement of the filter is the origin of the high frequency fluctuations on the waveforms [20]. In such FDML fiber laser cavities with nonzero dispersion, the triggering of Eckhaus instability is unavoidable. Some attempts have been tried to enhance the coherent length. Discretization of the swept spectrum into small sections by a comb filter is demonstrated effective to enhance the coherent length by several times [19, 21, 22]. But such fixed comb filter will introduce a limitation of the detection depth of OCT by the round trip time of the Fabry-Pérot (FP) filter.

It is not easy and not cost-effective to fabricate multiple comb filters with different free spectral ranges and linewidths [21].

In this paper, we propose a novel discretization method of the FDML signal with an intracavity intensity modulator. In Section 2, we theoretically demonstrate the similarity and difference of the spectral slicing with comb filter and temporal intensity modulation that applied to a wavelength swept signal. Then we adopt the intensity modulator jointly with a comb filter to realize a time and Fourier domain jointly mode locked (TFDML) fiber laser in Section 3. Conclusions are drawn in Section 4.

2. Principle of discretization of swept signal

When an FP etalon is inserted into the cavity of an FDML fiber laser, the spectral amplitude of the swept signal will be filtered by a transfer function

$$\tilde{H}(\omega) = \frac{1-R}{1-Re^{i\omega\tau}}, \tag{1}$$

where R is the intensity reflectivity of the facet of the FP etalon, τ is the round trip time in the FP cavity. $\tilde{H}(\omega)$ is a periodic function with a free spectral range (FSR) of $2\pi/\tau$. A comb like spectrum will be obtained after the filtering. If the input signal is linearly chirped as

$$A(t) = A_0(t)e^{-iat^2/2}, \tag{2}$$

where a is the chirp factor and also the sweep slope of the swept signal with central frequency $\omega_0(t) = \omega_0(0) + at$, the filtering will introduce a periodic modulation on the temporal waveform accordingly. If we consider a comb filter with a linewidth much larger than the instantaneous linewidth and a slow sweeping, then the temporal intensity modulation can be approximately written

$$H(t) = \frac{(1-R)^2}{1+R^2 - 2R\cos\{[\omega_0(0)+at]\tau\}}. \tag{3}$$
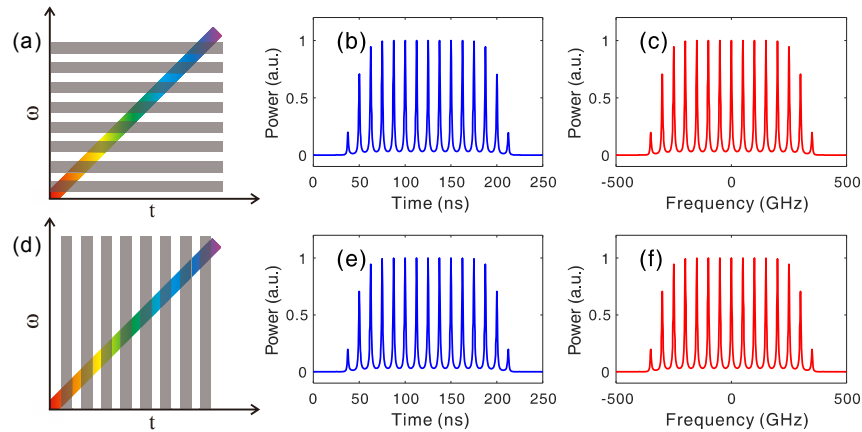

Fig. 1. The principle of (a) filtering by a comb filter and (b) modulation with a periodic function of a linearly chirped signal. (b) and (c) show the temporal and spectral profiles of the swept signal after the filtering. (e) and (f) show the temporal and spectral profiles of the swept signal after the modulation.

In Fig. 1(a), we illustrate the principle of such filtering. The truncation of the chirp signal by the comb filter will simultaneously chop the signal on time domain since the signal with different central frequency arrives the filter at different time. Comb structures are observed on

both the temporal waveform and spectrum as shown in Figs. 1(b) and 1(c) respectively, where a linearly chirped signal with a SuperGaussian envelope $A_0(t) = \exp[-0.5 \times (3t/T)^{10}]$ is used as the input. The sweep duration T is 100 ns and the sweep slope a is $4\pi \times 10^{18}$ s^{-2} in Fig. 1. The FP etalon has an FSR of 50 GHz and reflectivity $R = 0.6$.

The temporal modulation on the waveform shown in Fig. 1(b) implies an alternative mechanism to obtain similar discretization of the signal besides the filtering. When a temporal intensity modulation is applied on the linearly chirped SuperGaussian swept signal, the spectrum will be sliced too, as illustrated by Fig. 1(d). Figures 1(e) and 1(f) show the corresponding temporal and spectral profiles after a temporal intensity modulation but not filtering. Very similar temporal and spectral profiles are obtained with intensity modulation and spectral filtering, as shown in Figs. 1(b), 1(c), 1(e) and 1(f). Such equivalence of the spectral filtering and temporal modulation is valid when the condition $\Delta\omega\Delta t \gg 1$ is satisfied, where $\Delta\omega$ and Δt are the filter linewidth and pulse duration of the modulation respectively with a relation $\Delta\omega = a\Delta t$. It should be noted that the filtering and modulation will lead to some different features if the swept signal is not a smooth signal but has a large instantaneous linewidth or equivalently high frequency fluctuations on the waveform.
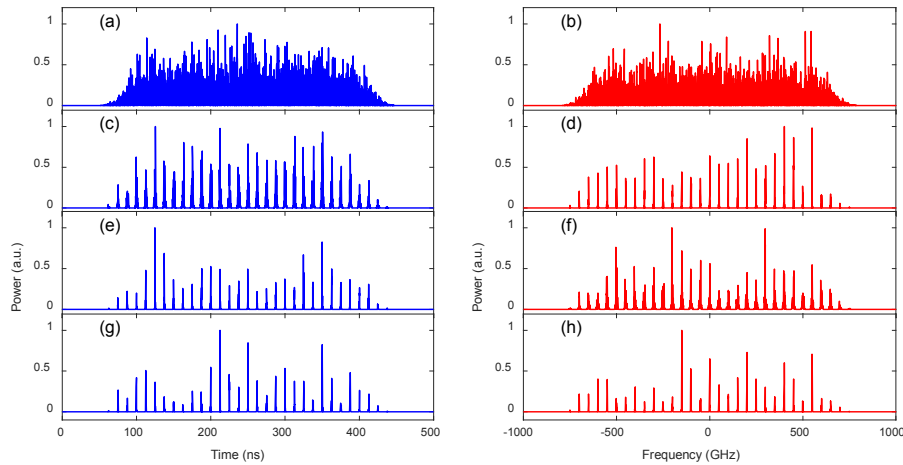

Fig. 2. The (a)(c)(e)(g) temporal and (b)(d)(f)(h) spectral profiles of the signals (a)(b) linearly chirped with a 5 GHz Gaussian line shape, (c)(d) filtered 3 times, (e)(f) modulated 3 times, and (g)(h) iteratively filtered and modulated 3 times.

We use a swept signal with a finite linewidth to investigate the performance of the filtering with an FP etalon and the periodic modulation. The input signal has a Gaussian instantaneous line shape modeled as

$$A(t) = \mathbb{F}^{-1}\left[e^{-\frac{1}{2}(\omega/\omega_l)^2 - i\phi(\omega)} \right] e^{-\frac{1}{2}(3t/T)^{10} - iat^2/2}, \tag{4}$$

where the linewidth ω_l is 5 GHz and $\phi(\omega)$ is a uniformly distributed random number in [0 2π], the sweep duration $T = 500$ ns and $a = 8\pi \times 10^{18}$ s^{-2}. $\mathbb{F}$ denotes the Fourier transform. Figure 2 shows the temporal waveforms and spectra of the input signal and output signals after filtering, modulation and their combination. The curves in Figs. 2(a) and 2(b) are respectively the waveform and spectrum of the input signal. Both the waveform and spectrum of the input signal are very noisy. The signal shown in Figs. 2(c) and 2(d) has passed the FP comb filter for 3 times. The spectrum has been sliced into multiple comb lines and all of the comb lines are well narrowed by the spectral comb filter. Unlike the narrow comb lines on the spectrum, although the waveform is also sliced into multiple comb lines, the linewidths are not well narrowed since there is no direct temporal shaper such as modulator that was applied to the signal. Such phenomenon is also observed when the modulation is applied to the signal by 3

times, as shown in Figs. 2(e) and 2(f). The linewidths of the spectral comb lines in Fig. 2(f) are obviously larger than that in Fig. 2(d).
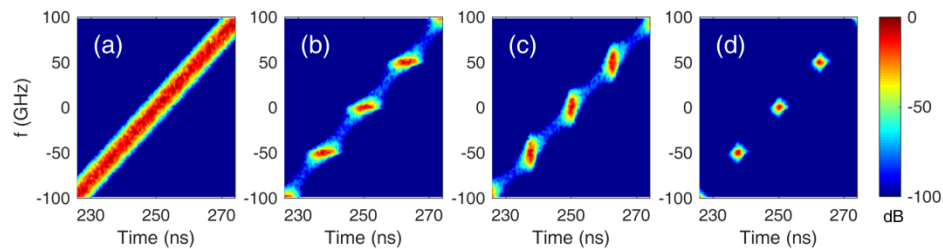

Fig. 3. Spectrograms of the (a) input signal, (b) filtered signal, (c) modulated signal and (d) jointly filtered and modulated signal.

To demonstrate the different features of the waveform and spectrum, we plot the spectrograms of the signals in Fig. 3. The input, filtered, modulated signals are plotted in Figs. 3(a), 3(b) and 3(c) respectively. The spectrograms are generated by Fourier transforms after applying a 0.61 ns Chebyshev gating window centered at different temporal position of the signals. The corresponding frequency resolution of the spectrograms is 0.75 GHz. In the spectrograms, both the filtering and modulation have sliced the continuous band of the input signal into discrete elliptical spots. The spectrograms of the filtered and modulated signal have longer traces in time and frequency domain respectively. All of the elliptical spots in Figs. 3(b) and 3(c) are significantly irregular due to the noise in the signals. From the spectrograms, the qualities of the signals after filtering and modulation have no much difference. To improve the signal quality, the FP comb filtering and the modulation are jointly used, as shown in Figs. 2(g), 2(h) and 3(d). The filtering and modulation are successively and iteratively applied to the input signal for 3 rounds. From Figs. 2(g) and 2(h), both the temporal and spectral comb lines are well narrowed. The quality of the spots in the spectrogram shown in Fig. 3(d) is significantly enhanced comparing with those in Figs. 3(b) and 3(c).

3. Experimental realization of TFDML fiber laser

3.1 Experimental setup

The analysis in Section 2 indicates that both a comb filter and a periodic modulation applied in the cavity discretize the chirped signal in temporal and frequency domain simultaneously. When the chirped signal has a relative large instantaneous linewidth, the joint using of the comb filter and the temporal modulation will be a better choice to improve the signal quality. Because of the unavoidable dispersion and hence mismatch between the sweeping period and the round trip times of signals with different wavelength, a relative large instantaneous linewidth are generally observed for the signal of FDML fiber lasers. It has already been demonstrated that an FP comb filter is effective to improve the signal quality and enhance the coherence length of the output signal. In this section, we will experimentally investigate the signal quality enhancement by jointly applying the FP comb filter and a modulator in the FDML fiber laser cavity. Such simultaneous temporal and spectral chopping to the intracavity signal leads to a time and Fourier domain jointly mode locked fiber laser.

Figure 4 shows the schematic diagram of a TFDML fiber laser with a comb filter and a modulator in the cavity. Two semiconductor optical amplifiers (SOAs) are used as the gain medium to compensate the cavity loss. The wavelength sweeping is realized by the periodic scanning of a fiber FP tunable filter (FFP-TF). The FFP-TF has an FSR of 200 nm and a linewidth of 16 GHz. An FP comb filter (FP-CF) with an FSR of 50 GHz, which is markedly larger than the linewidth of the FFP-TF, is used to discretize the sweeping spectrum. As the unique component of FDML fiber laser, a section of dispersion shifted fiber (DSF) in

kilometers length is inserted into the cavity to buffer the sweeping signal. The FFP-TF is driven by a periodic signal generated by an arbitrary waveform generator with a period equal to the roundtrip time of the long fiber cavity. Isolators (ISOs) and polarization controllers (PCs) are used to avoid the backward propagation and adjust the polarization state of the signal. 50% of the power is coupled out of the cavity after the FFP-TF. An intensity modulator (MOD) and a 5% coupler to extract the signal as the trigger of the modulator are inserted into the cavity after the FP-CF.
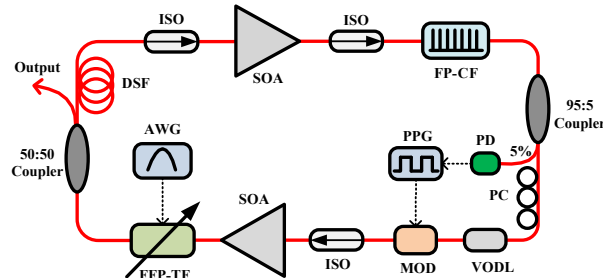

Fig. 4. Schematic diagrams of TFDML fiber laser with a comb filter and a modulator in the cavity.

In principle, it is possible to use the intensity modulator solely to get discrete swept signal. But such configuration is currently hard to maintain the k-space linearity of the discretized signal because of the nonlinear sweeping of the FFP-TF, which is normally driven by sinusoidal signals. Another challenge to use the modulator individually is the synchronization of the low repetition rate driving signal of the FFP-TF and the high repetition rate driving signal of the modulator. Such challenges are believed to be solved in further engineering of the signal generation in the future, but it is more convenient to obtain a naturally synchronized pulse train to drive the modulator by detecting the signal sliced by an intracavity FP comb filter or other periodic filters such as Mach-Zehnder interferometer in a illustrative realization. With the intracavity comb filter, the discretized signal will be uniformly distributed in frequency domain.

In the running cavities, the signal from the lower SOA in Fig. 4 will be dynamically filtered to a swept signal in the FFP-TF driven by a sinusoidal electrical signal at a fixed frequency. It should be noted that the choice of driving frequency is limited in a narrow band around the resonant response frequency of the piezoelectric transducer (PZT) in the FFP-TF. After the coupler, 50% of the swept signal is injected into the DSF, which has a delay time equal to the sweep period of the FFP-TF. Another SOA is following the DSF to compensate the loss of the FFP-TF, coupler and DSF. The amplified signal is then injected into the FP-CF, where the spectrum will be sliced with frequency spacing accordant to the FSR. As illustrated in Figs. 1-3, the filtering will lead to a periodic temporal modulation to the signal. 5% of such a pulsed swept signal will be coupled out and detected by a photodetector (PD). The electrical pulse signal will trigger a programmable pulse generator (PPG) to generate an ultra-short driving pulse train with a tunable delay to drive the modulator. The residual part of the swept optical signal will be modulated by the modulator to improve the quality. Since the modulator is polarization dependent, we use a PC to adjust the polarization state of the light. To synchronize the driving signal of the modulator and the optical signal, a variable optical delay line (VODL) is inserted before the modulator. The modulated swept optical signal will be injected into the lower SOA to start another round trip.

3.2 Results and discussion

The FFP-TF (Micron Optics) used in our experiment has a resonant frequency near 43 kHz. In experiment, the fiber cavity has a length of 4.753 km including the long DSF, which corresponds to a round trip time of 23.3 μs and a sweep rate of 42.94 kHz. The FFP-TF is

driven to sweep in a range of 41 nm. An FP-CF with an FSR of 50 GHz and a finesse of 12.6 is used to slice the spectrum. The sliced signal coming out from the 5% coupler is detected by a PD (Thorlabs PDB570C) and then used to trigger a digital delay/pulse generator (DDG, Stanford Research Systems DG645) to generate the driving signal to the modulator. The DDG generates ultrashort pulses with 10 ns pulse width triggered by the input pulse signal. The ultrashort pulse train captured in one period of the sweeping signal is shown in Fig. 5(a). The two vertical dashed lines indicate the starting and ending points of the period. The delay time of the output pulse train from the DDG can be adjusted in several μs with 1 ns resolution. The synchronization of the driving signal of the modulator and the input optical signal are further adjusted with the VODL, which provides a picosecond level resolution. The output waveform from the TFDML fiber laser is shown in Fig. 5(b). The region between the two vertical dashed lines is a whole period of sweep. The temporal waveform is discretized into narrow pulses by the comb filter and modulator. The temporal separation of the pulses are not identical since the sweep function of the FFP-TF is sinusoidal thus the sweep slope near the borders of the sweep region is much lower than that in the central part.
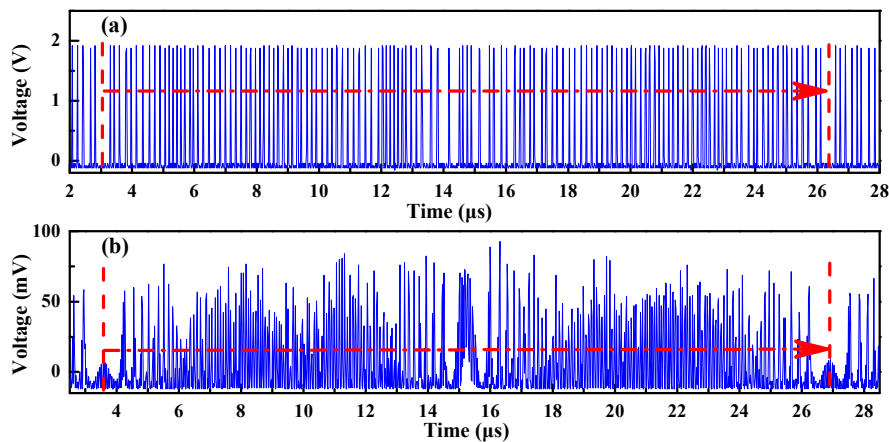

Fig. 5. (a) The driving signal of the modulator generated by the DDG. (b) The temporal waveform of the output signal from the TFDML fiber laser. The regions between the vertical dashed lines are in a whole period of sweep, which is 23.3 μs.

We can observe the detail of the waveform more clearly in in Fig. 6(a), where only half a period of the sweep is plotted. The variation of the separations between adjacent pulses along the sweeping is clearly observed. The separation is rather large at the beginning, where the FFP-TF locates at the border of the sweep range and the sinusoidal driving signal has a zero slope. Along the sweeping, the separation decreases to the minimum at the center part when the FFP-TF locates at the center of the sweep range and the largest slope of the sinusoidal driving signal is reached. The discrete short pulses in Fig. 6(a) have different central wavelengths, which correspondences to the spectral comb lines shown in Fig. 6(b) one-to-one. Thus the short pulses have an identical wavelength separation ~0.4 nm despite of the very different temporal separations. Although the intensities of the pulses in Fig. 6(a) fluctuate significantly, the integrated discretized spectrum shown in Fig. 6(b) is very smooth and stable. The power fluctuation of the pulse corresponding to each comb line in different round trips has been greatly reduced by averaging in the long detection period. Since the output pulses of the TFDML fiber laser have the same frequency spacing, it is convenient to use the signal simultaneous as the probe and clock in OCT system to obtain the interfered spectrum directly without any remapping of the signals.
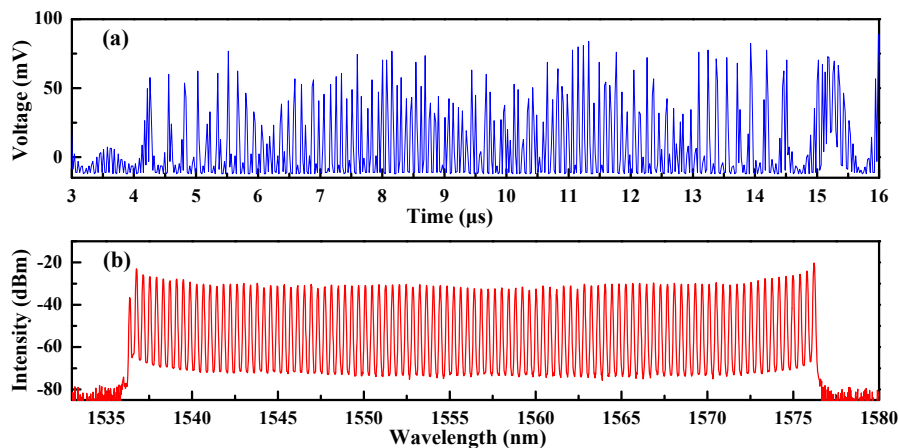
Fig. 6. (a) The temporal waveform in half a period of the sweep and (b) the spectrum of the output signal of the TFDML fiber laser.

Similar to the results in [21], the coherence length of a discretized FDML is improved when compared to that of conventional FDML. However, besides improving the signal quality, such discretization of the swept signal also introduces an additional limitation to the detection length in OCT applications because of periodic aliasing of the signals [21]. The maximum detection length is limited to ~1.5 mm by the 50 GHz FSR of our laser. To enhance the detection length, a comb filter with much smaller FSR should be used. Since the coherence length of conventional FDML fiber lasers is already longer than the FSR-limited detection length [21], quantitative estimation of the coherence length enhancement will be possible only when a high quality comb filter with an FSR close to or smaller than 10 GHz is available. One can also achieve such dense discretization by using an intensity modulator, which is a more flexible method than using comb filter but the driving signals of the FFP-TF must be synchronized with the modulator first.

4. Conclusions

In this paper, we propose a novel discretization method of the FDML signal with an intracavity intensity modulator. With numerical simulations, it is found that the discretization of a linearly chirped signal can be realized with a comb filter and/or a periodically driven intensity modulator. Simulations also show that the jointly using of comb filter and intensity modulation to the noisy swept signal will improve the signal quality. Based on such method, we proposed and successfully demonstrated a time and Fourier domain jointly mode locked fiber laser in experiment. Discrete wavelength swept laser output with a wavelength spacing of ~0.4 nm in a 41 nm sweeping range is achieved. The scheme of discrete FDML fiber laser using intensity modulator solely is also a promising and more flexible method to replace the comb filter scheme if the synchronization of the driving signals of the FFP-TF and modulator is guaranteed with further engineering.

Funding